Engineering and Technology Journal
Journal homepage: https://etj.uotechnology.edu.iq

Effect of friction stir processing of in-situ A356/Al_3Ni composites: microstructure refinement and wear behavior

Noor A. Baheer[a]*, Muna K. Abbass[a], Israa A. Aziz[a], Fuad Khoshnaw[b]

[a] Production Engineering and Metallurgy Dept., University of Technology-Iraq, Alsina'a street, 10066 Baghdad, Iraq.
[b] School of Engineering and Sustainable Development, De Montfort University, United Kingdom.
*Corresponding author Email: pme.20.40@grad.uotechnology.edu.iq

HIGHLIGHTS

- A356/Al_3Ni in-situ composites were fabricated using the stir casting method.
- FSP enhanced the microstructure by refining grains in A356 and the in-situ composite.
- FSP increased hardness to 87 HV for A356 and 173 HV for the A356/Al_3Ni composite.
- The A356/Al_3Ni composite after FSP showed superior wear resistance over the base and pre-FSP composite.

Keywords:

Al-alloy A356
Stir casting
Friction stir processing
In-situ composite Al_3Ni
Wear rate

ABSTRACT

This research investigated the impact of friction stir processing on grain refinement in the surface layer of composite materials. The in-situ composite was created by stir casting, incorporating 15% pure Ni into the Al matrix type A356. Microstructural analysis performed with optical microscopy and X-ray diffraction revealed the formation and dispersion of intermetallic phases such as AlNi, Al_3Ni, and Al_3Ni_2, contributing to significant grain refinement. FSP further enhanced the micros structure by breaking and uniformly distributing small particles, including the primary Si phase and Al_3Ni, while refining α-Al dendrites. These microstructural changes resulted in improved mechanical properties, including a 13.81% increase in hardness for the A356/Al_3Ni composite and a 14.47% increase for the base A356 alloy. Wear rate tests were conducted using a ball-on-disc apparatus under dry sliding conditions for both the base alloy A356 and the in-situ composite A356/Al_3Ni, before and after FSP. Compared to the base alloy A356 and in situ composites before and after friction stir processing, the in-situ composite (A356/Al_3Ni) after FSP exhibited a lower wear rate. However, during the wear test, the coefficient of friction decreased as the applied load increased for the base alloy A356 and the in-situ composite (A356/Al_3Ni) following the friction stir process.

1. Introduction

The automotive and aerospace industries play a significant role in the rise of high-strength aluminum alloys. Electronic packaging, power transmission towers, aircraft, internal combustion engine components, and various other products are among the most promising applications of Al alloys [1]. The term Aluminum Matrix Composites (AMCs) refers to a specifically engineered combination of aluminum (matrix) with either matrix or rigid reinforcement (the matrix contains the reinforcing material). Numerous manufacturing processes have continuously evolved to enhance the mechanical properties and microstructure of AMCs. Since the manufacturing process directly impacts the properties of the finished product, it is an essential part of creating AMCs. Solid- and liquid-state fabrications and in-situ-state fabrication are all included in the general category of ex-situ fabrication techniques for AMCs [2]. The dispersed phases may be either generated internally or introduced as an external phase in metal matrix composites (MMCs), and both methods present their advantages and disadvantages. The term "ex-situ" describes a method in which a dispersed phase is synthesized individually before being added to the matrix [3]. In situ synthesis methods have been employed to address this issue, enhance the thermal stability of dispersed reinforcement particles in the matrix, and improve matrix-reinforcement wettability. In-situ approaches boost the adhesion at the interface and, therefore, the mechanical characteristics [4].

Furthermore, the in-situ technique has the benefits of being isotropic, having an even particle distribution of reinforcement within the metallic matrix, and having an effective chemical interaction between the matrix and the reinforcement phase [5]. The stir casting technique employs a mechanical stirrer to generate a vortex in the matrix material to incorporate reinforcement. The main advantages of stir casting are versatility, ease of use, and potential for large-scale production [6]. The microstructure of A356 in the as-cast condition is usually identified by a massive dendritic structure, which includes porosity and Si particles that

http://doi.org/10.30684/etj.2025.156833.1887
Received 09 March 202; Received in revised form 22 April 2025; Accepted 14 May 2025; Available online 14 September 2025
2412-0758/University of Technology-Iraq, Baghdad, Iraq

are irregularly distributed in the spaces between the dendrites [7]. Friction stir processing, or FSP, was investigated to eliminate some obstacles associated with casting A356. The FSP process breaks and refines particle agglomerates, intermetallic compound particles, and dendritic forms by applying a rotating tool with a probe, causing considerable deformation induced by frictional heating. Porosity is closed or refined to improve the mechanical properties [8,9]. The main uses of FSP are modifying the microstructure of metallic materials, enhancing plasticity, achieving homogeneity in aluminum alloys and AMMCs, refining the microstructure of cast aluminum alloys, creating metal foam, and constructing ex-situ and in-situ composites [10,11].

Aktarer et al. [12], thoroughly investigated the impacts of single-pass FSP on the Al-12Si basic alloy and its implications for wear and friction properties. During FSP, intense plastic deformation and dynamic recrystallization break down the needle-shaped eutectic silicon particles, leading to a more uniform distribution. This refinement enhances the alloy's mechanical strength and wear resistance. The study also analyzes the wear mechanisms and discusses possible reasons for the observed improvements. Friction stir processing for strengthening industrial waste particles in cast A356 alloy was studied by Kumar et al. [13], addressing common issues in melt-based composite fabrication, such as particle aggregation, poor wettability, and harmful phase formation. FSP improved the alloy's microstructure by eliminating porosity, refining grains, breaking and redistributing Si particles, and fragmenting α-Al dendrites. The resulting composite showed a uniform distribution of reinforcement without detrimental phases at the particle/matrix interface. Mechanical and wear properties, including strength, ductility, and wear resistance, were significantly enhanced compared to the as-cast alloy due to these microstructural improvements. Daneshifar et al. [14], manufactured Al/Mg_2Si in-situ composites using FSP. FSP injected pure magnesium into an Al-Si casting eutectic alloy. A variety of analytical techniques were used to study Mg_2Si formation. The production of Mg_2Si was investigated using several analytical methodologies. The findings demonstrate a notable increase in hardness (~15%) and a uniform dispersion of the Mg_2Si particles. Samal et al. [15], investigated the sliding wear behavior of SiC-reinforced composites. The 15 wt.% SiC composite's wear rate was 51% lower than the base alloy's at 2000 m of sliding distance and 66% lower at 30 N when a force of 10 N was applied. Gautam et al. [16], used the cooling slope method to investigate the mechanical characteristics and wear of on-site A356/5%TiB_2 composite synthesis. It was discovered that adding TiB_2 particles improves the mechanical characteristics of the cast composite material. The TiB_2 content considerably reduces the composites wear rate. Examining the worn surface indicates that plowing and adhesion are the leading causes of surface wear. Singhal et al. [17], produced AA5083-H111/Al-Fe surface composites through in-situ processing. A two-step friction stir process altered the tool's motion while producing the AA5083 substrate. After the first run, the ultimate tensile strength was 225.8 MPa; after a second pass, it was 253.6 MPa. Furthermore, microhardness was 128.3 HV after the second run and 123.3 HV after the first, using multi-pass FSP. Rubtsov et al. [18], investigated the use of multi-pass friction stir processing (FSP) to incorporate 1.5–30 vol.% copper powder into an AA5056 aluminum matrix to form an in situ composite reinforced with Al-Cu intermetallic compounds (IMCs). Initial FSP passes resulted in macrostructural inhomogeneity, which improved with additional passes. During FSP, copper agglomerates were compacted and saturated with aluminum, forming various phases such as α-Al(Cu), α-Cu(Al), Cu_3Al, CuAl, and S/S -Al_2CuMg precipitates. The formation of these IMCs increased with more FSP passes, leading to a 50–55% improvement in microhardness.

Because in-situ processing routes may surpass the technological challenges of ex-situ processing routes, they are frequently used to produce MMCs. The technical challenges include particle dispersion, interphase formation, and insufficient reinforcement bonding with the matrix material. The primary goal of this study was to use stir casting to generate an in-situ composite of A356 aluminum alloy reinforced with Al_3Ni particles. Then, the microstructure of the A356/Al_3Ni composite was refined in the stir zone created by FSP. Before and during friction, the base alloy and in-situ composite are examined for mechanical, tribological, and microstructural features.

2. Experimental work

The alloy utilized in the current research was A356 Al alloy, which is commercially manufactured from pure Al and an Al–11% silicon master alloy supplied by the General Company for Electrical Industries in Wazirya (Baghdad). All the used materials were melted at 750 °C in an electric furnace. Consequently, the molten alloy was poured into a metallic mold after being chemically modified. A Thermo ARL3460-type optical emission spectrometer was used to investigate the chemical composition of the manufactured aluminum A356. The chemical composition of Al alloy A356 is displayed in Table 1.

Table 1: Chemical composition of prepared A356 alloy

Element (wt.%)	Si	Fe	Cu	Mn	Mg	Zn	Ti	Al
Actual value measured	7.38	0.5	0.2	0.1	0.4	0.3	0.02	Balance
Standard value [13]	6.6-7.5	0.6	0.25	0.35	0.20-0.45	0.35	0.25	Balance

2.1 Fabrication of Al_3Ni in-situ composites by stir casting

In-situ composites of Al_3Ni were created by combining nickel (15 weight percent) with aluminum alloy A356 (China Jingan Chemicals and Alloys Limited) as the matrix and using 1.0175 μm particles as reinforcement. Aluminum alloy A356 was deposited in an alumina crucible at 750 °C, above the liquidus temperature, using an electric furnace. To remove impurities (such as slag), flux (1% CaF_2) was added to the melt after homogenizing it at this temperature for approximately 15 minutes. Effective reinforcing dispersion within the melt and degassing was achieved utilizing an inert gas (argon). Ni particles were introduced, twisted in aluminum foil, and warmed to 350 °C for 1 hour to remove moisture. As shown in Figure 1, an electrically powered stirrer set at 500 rpm was used to gradually add Ni particles to the melted alloy. A rectangular metallic mold (10 × 100 × 150 mm^3) heated to 250 °C was filled with the molten alloy.

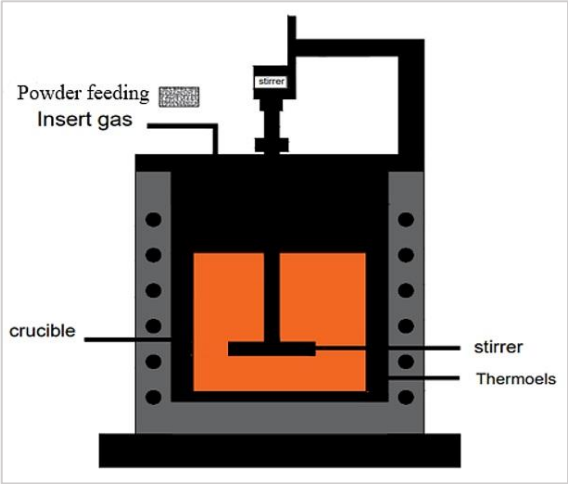

Figure 1: Stir-casting method

2.2 Friction stir processing (FSP)

Numerical analysis was carried out utilizing a computer-controlled vertical machining center (Knuth Werkzeugmaschinen GmbH, Germany) to determine the optimal settings for FSP. A 1250 rpm fixed rotation speed, 3.1 mm plunge maximum depth, and 75 mm/min travel velocity were selected since several trials were conducted at room temperature (one pass). Tool steel type X12M was used to design and manufacture the FSP tool. The geometric shape comprises a 6 mm diameter pin, 3 mm depth, and 16 mm shoulder.

2.3 Specimen preparation

The microstructure of the materials was characterized by being examined under an optical microscope. Freshwater and SiC (silicon emery paper in grits of 320, 500, 600, 800, 1000, and 1200) were used for wet grinding. The sample was polished using an appropriate lubricating cloth with 0.5 µm diamond paste. Keller's substance, which is a solution of 95 ml H_2O, 2.50 ml HNO_3, 1.50 ml HCl, and 1 ml HF, was used to etch the specimens. After being cleaned, these specimens underwent a procedure to remove humidity.

The VEGA3LMe model, a high-resolution image scanning electron microscopy (SEM) instrument, was employed. The Vickers hardness test was performed using the Laryee HVS-1000 digital micro-hardness tester by exerting 200 grams of force on the shoulder for 15 seconds. Dry sliding wear was studied using the ball-on-disc wear test standard (G99) concept with a radius of 3 mm and 250 rpm. The loads (5, 10, 15, and 20 N) were applied for a specific duration (20 minutes). The 10 × 15 × 15 mm^3 specimen was weighed with an accuracy of 0.0001T on an electronic balance before the test. The tested specimen was weighed again later. The friction coefficient (µ) was measured using this device under various loads.

3. Results and discussion

3.1 Microstructure

Figure 2a shows a micrograph of the base alloy A356 after FSP. Four different zones were identified in the FSP specimen. The stir zone (SZ), a thermomechanically treated area, is characterized by an equiaxed or homogenized structure and fine particle size. The three zones are the thermomechanically affected zone (TMAZ), the heat-affected zone (HAZ), and the FS-treated zone. Thermomechanical deformation causes the TMAZ to have enlarged grains. The HAZ and the base metal (BM) share a similar grain structure. BM is the area unaffected by the FSP. Thermomechanical deformation caused the grain in the TMAZ to expand. The grain structure of the HAZ is similar to that of the base metal (BM).

Base metal (BM) refers to the area not impacted by the FSP process. White spots in the dendritic morphology of A356 Al alloy demonstrate the existence of the main α-Al phase. Al-Si eutectic, which manifests as black areas, is also present. While silicon particles split into asymmetrical pieces inside the base metal, the eutectic phase surrounds α-Al dendrites continuously, as seen in Figure 2b. Following the FSP approach, the microstructure completely transforms, producing the expected altered structure. Figure 2c illustrates the significant and severe plastic deformation that occurred in the dendritic microstructure of the matrix alloy prior to refining. The FSP was used to refine the grains and alter the silicon. The SZ, which had a globular structure with small silicon particles, showed changes in microstructure. In the SZ, these particles have been distributed somewhat more evenly. The material experiences significant plastic deformation during friction stir processing at elevated temperatures in the stir zone. Nucleation sites were created during dynamic recrystallization when the material had been subjected to high temperatures.

The findings align with a study by Jlood et al. [19], which examined how FSP parameters affected the T6 mechanical and microstructural characteristics of the AA6061 alloy. It was found that the grain size of each pass is uniform in the large-area stir zone of the FSP, where fine equiaxed grains are generated. Similar findings were made by Ma et al. [20], who altered the as-cast microstructure of the cast A356 Al by using friction stir processing (FSP). FSP standardizes and enhances the cast microstructure, eradicates porosity, and produces a microstructure with diminutive Si particles (0.25–0.42 µm) dispersed inside a fine-grain aluminum matrix.

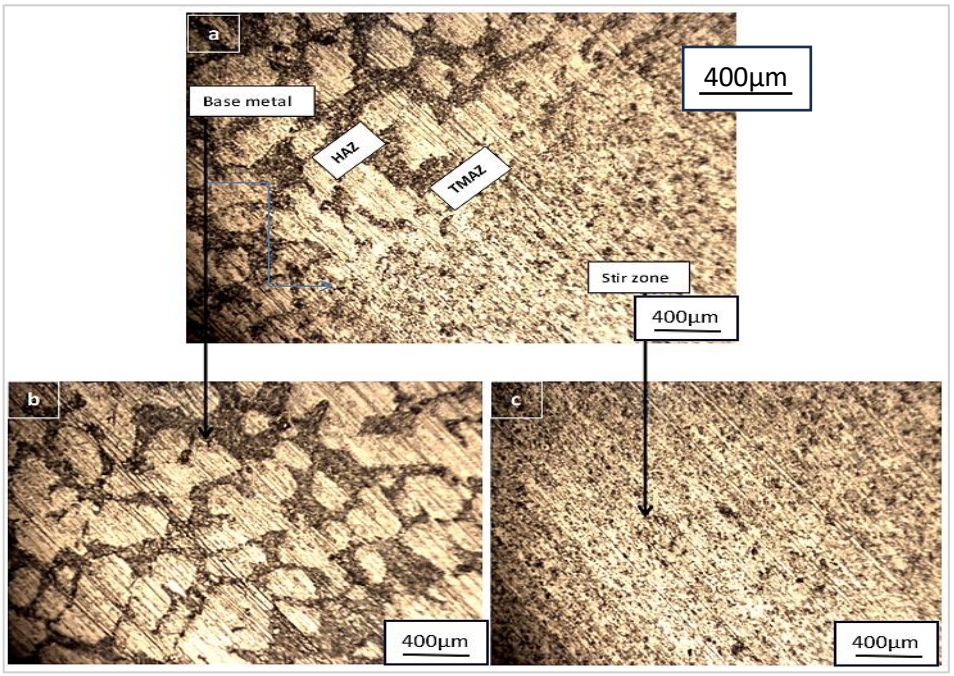

Figure 2: Optical micro-graphs showing micro-structure of the base A-356 alloy after FSP (a) The FSP zone: base metal, HAZ, TMAZ, and SZ at 400 × (b) The base metal at 400 × (c) SZ at 400 ×

The in-situ composites A356/Al_3Ni optical micrographs after FSP are shown in Figure 3a. There are four distinct zones observed: fine particle size and a homogenized or equiaxed structure, which are characteristics of the SZ, TMAZ, HAZ, and BM, which is the area that is unaffected by the FSP process. The in-situ composite consists of Al_3Ni, the intermetallic compound formed with a nonuniform distribution in the Al matrix, and clusters are also observed, as expected from Figure 3b. Figure 3c shows that different sizes of Al_3Ni particles, including fine and medium-sized ones, are uniformly dispersed throughout the matrix alloy in the stir zone following FSP. Additionally, various-sized and shaped Al3Ni intermetallic compounds were identified in the composites. These results align with the findings of Senthil et al., [21-23]. Similar findings were made by Zhao et al. [23], when they used FSP to attain super plasticity in in-situ nano-ZrB2/2024Al composites derived from the 2024Al-K2ZrF6-KBF4 system. They investigated the effects of deformation temperatures (400, 480, 600, 700, and 750 K) and particle concentrations (1, 3, and 5 wt.%) on composite super plasticity. The uniformity of the nano-ZrB_2 was enhanced by pulverizing the larger particles of the molded composites, and this had a matrix particle size of around 80–100 µm and a nano-ZrB_2 reinforcement length of 30-100 nm, into smaller grains of around one micrometer after friction-stir processing.

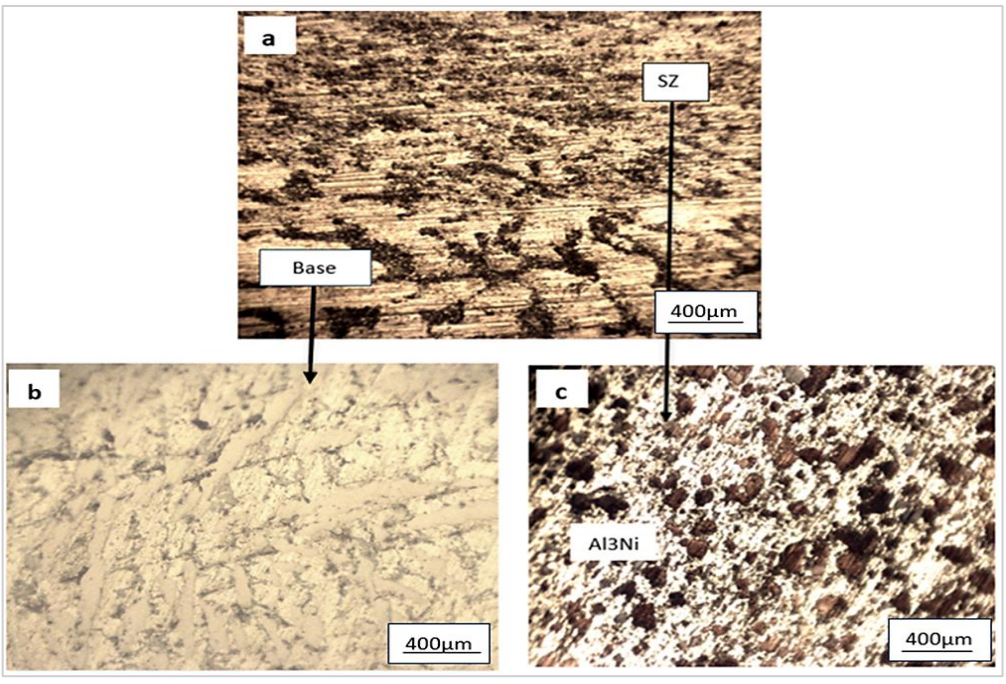

Figure 3: Optical micrographs showing micro-structure of in- situ composite A-356/Al3Ni after FSP (a) The FSP zone: base, TMAZ, HAZ, and SZ at 400 × (b) BM at 400× (c) SZ at 400 ×

Figures 4a and 4b provide SEM images depicting the morphology of the A356 alloy and in-situ composites comprising 15% nickel in their as-cast state without FSP. The initial microstructure of alloy A356, which is composed of two main Al-Si and α-Al eutectic phases, shows that a dendritic structure of the α-Al phase (the primary aluminum solid solution) is surrounded by a eutectic mixture of Al and Si (Al + Si). The eutectic phase appears as a network between the dendrite arms, as shown in Figure 4a. The distribution of Al_3Ni intermetallic compounds with various shapes and sizes of agglomeration of Al_3Ni intermetallic compounds has been observed in the 15wt.%Ni shown in Figure 4b. Figure 4c displays SEM pictures of the A356 cast microstructure following FSP. This method produced the refining of Al dendrites, the repositioning of tiny, identical Si particles inside the Al matrix, and the visible disintegration of fibrous Si particles. These results are in line with the ones by Kumar et al. [24], who discovered that during friction stir processing, the Eutectic Si needles were evenly distributed throughout the nugget zone in the matrix A356 alloy and had been transformed into fine spherical particles during FSP.

Figure 4d displays the microstructure of the A356/Al_3Ni AMC's friction-stir-processed zone, demonstrating a consistent distribution of Ni particles in Al_3Ni and A356 in-situ composites. FSP demonstrated complete uniformity. The revolving apparatus generates heat, while circumferential forces disseminate nickel particles over a wide area. This approach relates to the metal flow characteristics during the FSP of A356/Al_3Ni in-situ composites in the stir zone. A single FSP round enhanced dispersion and disrupted particle segregation at grain boundaries. These results have coincided with those reported by Dinaharan et al., [25]. Al_3Zr particle segmentation can be observed in AA6061/Al_3Zr DRAMC, whereas clusters of Al_3Ti particles were identified in AA6061/Al_3Ti DRAMC. The produced composites were put through FSP. The shape and distribution of the Al_3Zr and Al_3Ti particles experienced notable variations.

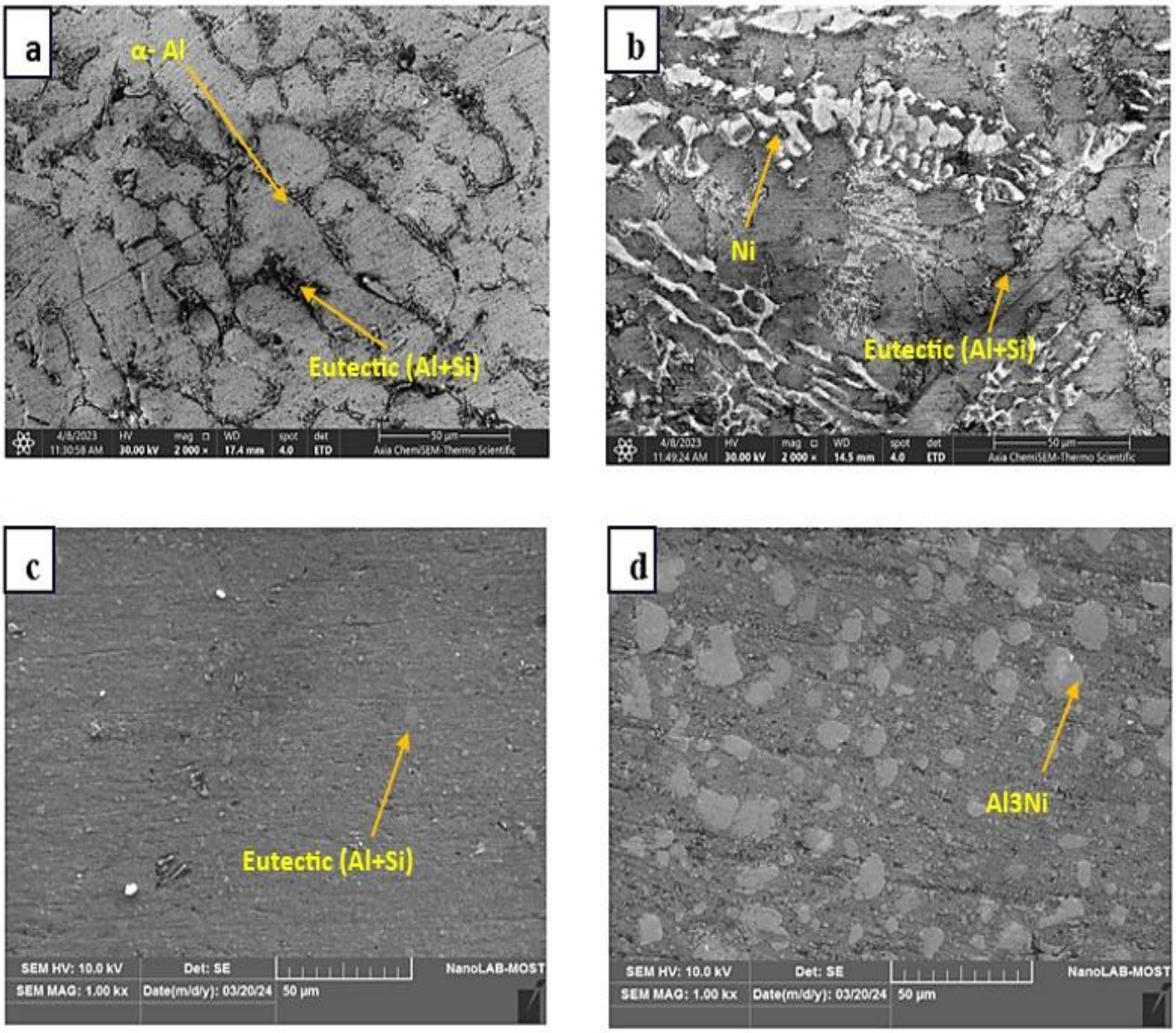

Figure 4: As cast A356SEM before and post FSP (a) A356 as cast, (b) A-356/Al_3Ni as cast, (c) A356 after FSP, and (d) A-356/Al_3Ni after friction stir processed

The dendritic structure of the base cast A356 is no longer discernible in the metal matrix following FSP, as shown in Figure 5 (a-e) demonstrates the microstructure and the distribution of Al, Si, Cu and Mg in stir zone of base alloy A356 respectively. The eutectic silicon particles were also reduced to smaller, evenly distributed spherical particles within the FSP zone.

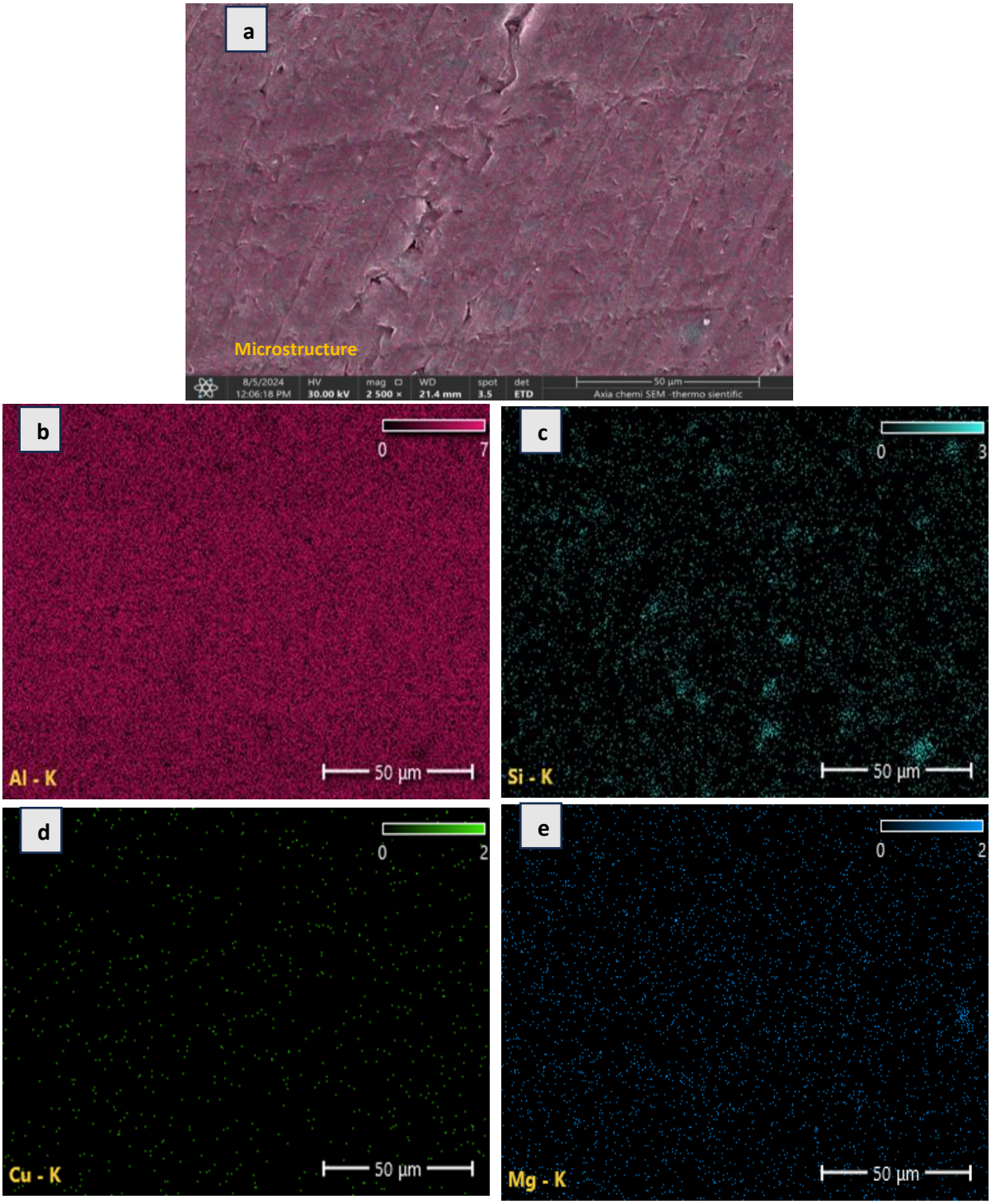

Figure 5: SEM-EDS elemental mapping for the stir zone of base alloy A356 after FSP (a, b, c, d and e) microstructure and distribution of Al, Si, Cu and Mg in stir zone of base alloy A356 respectively

The A356/Al_3Ni in-situ composite contains nickel particles in the FSP area of the stirring zone, as shown in Figure 6 (a-e) demonstrates the microstructure and the distribution of Ni, Mg, Al and Si in stir zone of the A356/Al_3Ni respectively. The particles of Al_3Ni are evenly distributed throughout the aluminum matrix. During FSP, all of the A356/Al_3Ni sample clusters disappeared. FSP causes the plasticized composite to experience high plastic strain, which degrades the Al_3Ni clusters. The FSP procedure altered the Al_3Ni particles shape and size. The various shapes of Al_3Ni particles are thoroughly fragmented into nearly spherical or fibrous-like shapes with different sizes.

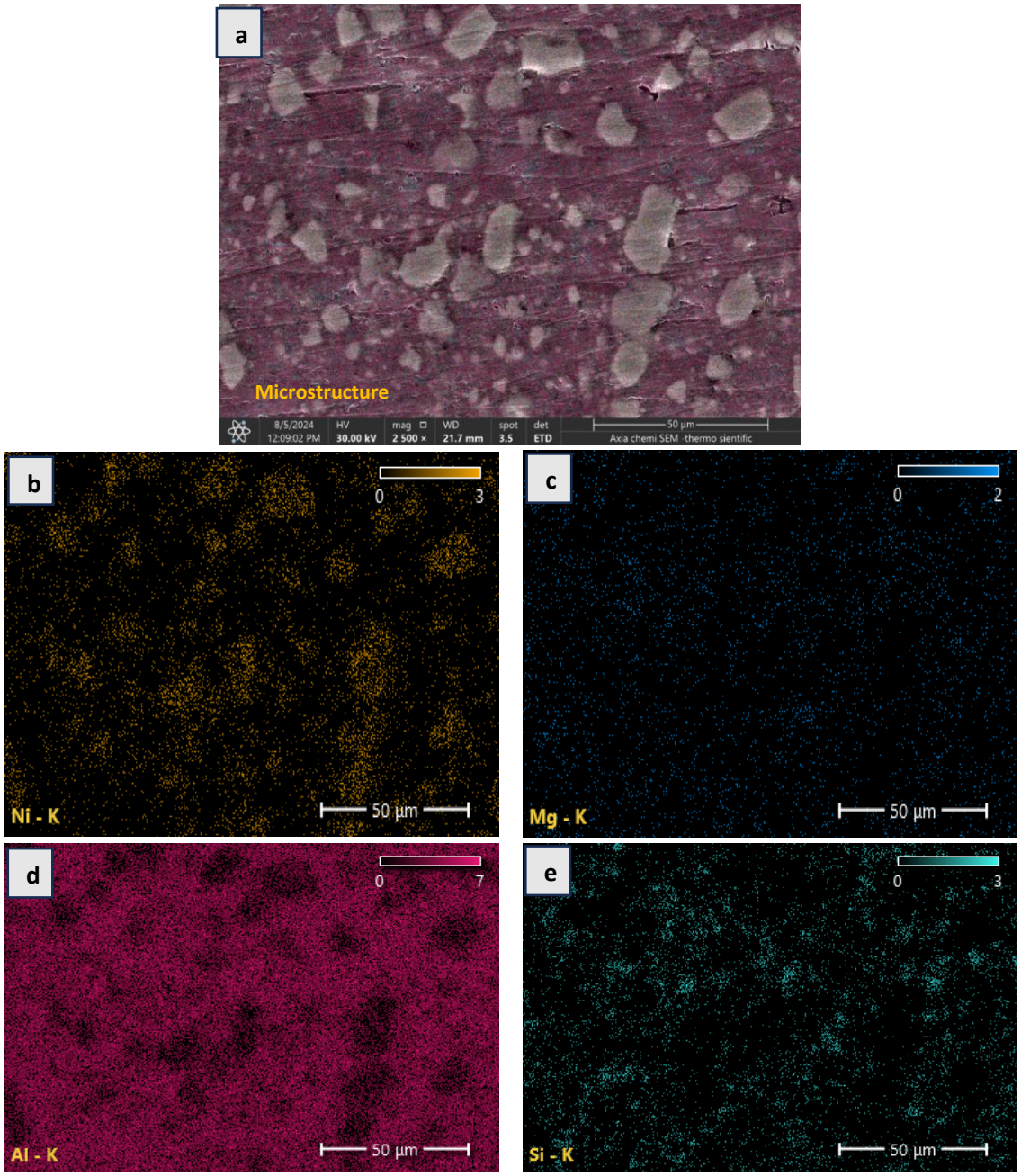

Figure 6: SEM-EDS elemental mapping for the stir zone of the A356/Al_3Ni after FSP (a, b, c, d and e) microstructure and the distribution of Ni, Mg, Al and Si in stir zone of the A356/Al_3Ni respectively

3.2 Microhardness

Figure 7 shows the specimens hardness profiles (A356 and A356/Al3Ni) before and after FSP. Each hardness value is determined by averaging at least three measurements. Because of refining grain and the dynamic recrystallized zone, hardness significantly rises after FSP. Before and after the first FSP pass, the as-cast A356 hardness was 76 and 87 HV, respectively, whereas the A356/Al3Ni hardness was 152 HV and 173 HV. For the A356/Al3Ni in-situ composite, the improved homogeneity of Al3Ni particle distribution after FSP leads to a more successful dispersion hardening. According to the Hall-Petch equation, high dislocation density and particle refinement improve hardness. These results align with the ones by Mohammed and Subhi [26], who used FSP to create SiC particles integrated into the surface of an A380 Al alloy across a range of processing conditions. The findings showed that during FSP, silicon was transformed into tiny globular particles dispersed throughout the stirring zone while the α-Al phase was refined. Within the stir zone, several SiC particles clustered together. According to silicon modification, α-Al reinforcement, and the inhibiting impact of SiC particles, deeper plunges produced increased hardness three times greater than the aluminum base. The combination of Al3Ni reinforcement and FSP results in the highest microhardness value, indicating a synergistic effect of these two treatments on the surface hardness of the material. Kurt et al. [27], created particle layer surfaces by combining SiC particles with commercially pure aluminum using friction stir processing (FSP). Specimens were exposed to different traverse rates and rotating tools with and without SiC powder. The findings demonstrated that the generated composite surfaces have three times greater hardness values than the aluminum base.

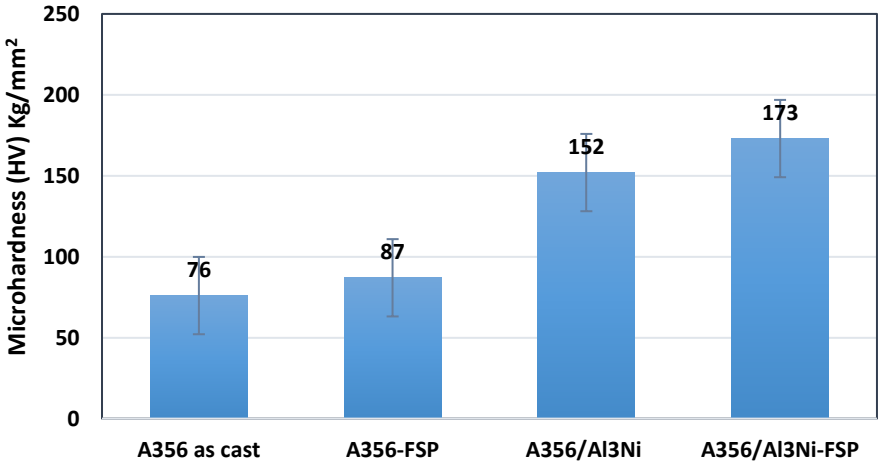

Figure 7: The microhardness values of the A356 alloy and the in-situ composites (A356/Al_3Ni) prior to and post-FSP

3.3 Tribological properties

3.3.1 Processing effects of friction stir on wear behavior

Figure 8 illustrates the relationship between applied load and wear rates for aluminum A356 as-cast and in-situ composite A356 (15% Ni) prior to and post-FSP. The ball-on-disc type was employed for wear testing, which was carried out under dry sliding circumstances with a test time of 20 minutes, a sliding distance of 90 meters, and an average sliding speed of 250 rpm. The rate of wear rises as the applied force increases for every specimen. This result is expected, as higher loads lead to greater contact pressure and more material removal. The addition of 15% nickel as an in-situ composite significantly improves the wear resistance of the A356 alloy. After applying FSP, the wear rate of the base alloy A356 and the in-situ composite A356 (15% Ni) significantly decreased compared to their pre-FSP state. The in-situ composite A356 (15% Ni) after FSP showed a lower wear rate, which was attributed to the increased hardness of the material caused by FSP. The intensive heat produced by FSP softens the matrix and ensures homogeneous Al_3Mg_2 distribution in the base A356 and Al_3Ni alloys in the A356 in-situ composite. FSP additionally promotes plastic deformation and microstructure refinement, which results in a harder, more wear-resistant material. The wear behavior under low loads (5 N) is either oxidative or moderate. According to Abbass et al. [28, 29, 30, 31], it changes into transition wear with loads ranging from 10 to 15 N before turning into metallic or severe at higher loads (20 N).

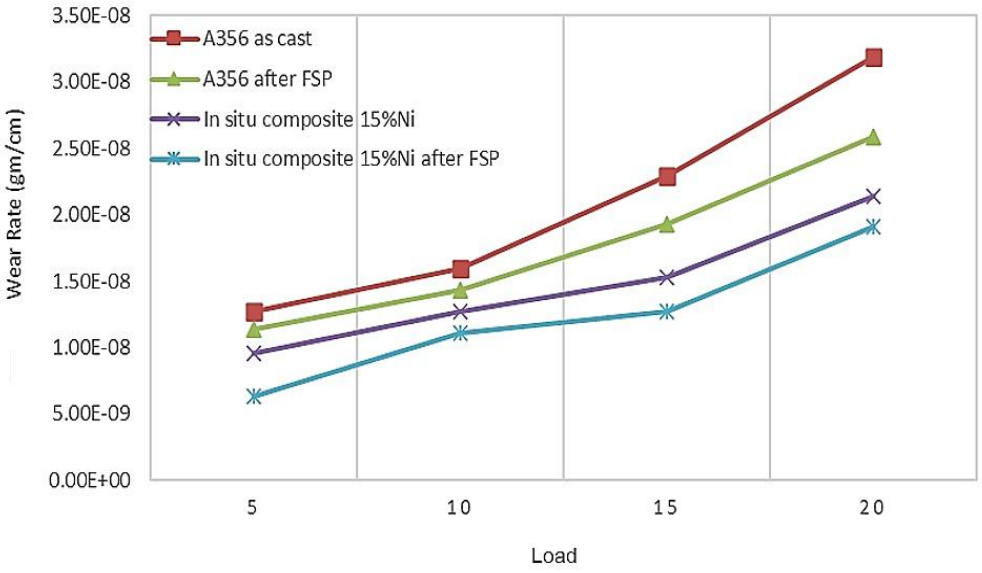

Figure 8: Effects of the applied load in (N) on wear rate for the base alloy A356 and the in-situ composite A356 (15%Ni) before and after the FSP

3.3.2 The worn surfaces topography

The SEM images of the base alloy A356 worn surfaces after FSP are displayed in Figure 9 (a, b). The plastic deformation and extensive material removal hardened the metal surface and created cracks, increasing the wear debris on the worn surfaces.

Wide and deep tracks, delamination, and grooves were observed on the worn surfaces at 20 N for 20 min. The image shows the presence of cracks on the worn surface. These cracks could have been initiated due to the stresses induced during the wear process, potentially exacerbated by the plastic deformation and the hardened surface layer (which might be more brittle).

Wear debris, consisting of small particles detached from the surface during wear, is scattered across the worn surface. These results are consistent with Shiba et al., [32]. The findings demonstrated that FSP considerably increased the wear resistance of A356 alloy surfaces. Compared to the as-cast A356 alloy, the frictional stir processed (FSP) treatment regions showed improved hardness, wear resistance, and reduced grain size. These findings align with other research [25, 33, 34].

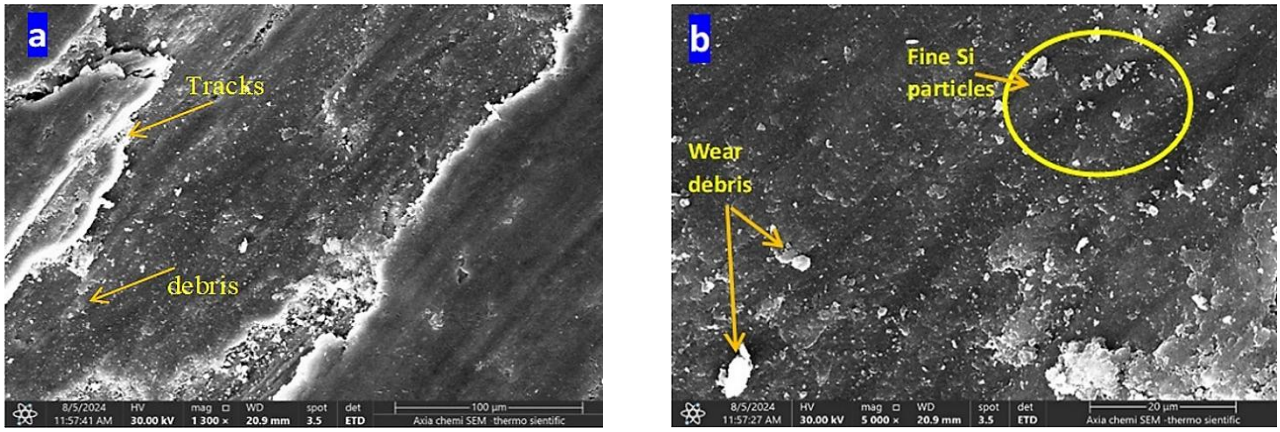

Figure 9: SEM images of the worn surface of FSP A356 after the wear testing at a load of 20 N for 20 min; (a) 100 µm, (b) 20 µm

SEM images of the cast A356 in-situ composite's worn areas following 20 N applied for 20 minutes are displayed in Figure 10 (a, b). Plastic deformation was not visible despite observing a parallel wear line or track. The in-situ synthesis of Al_3Ni restricts the material's plastic deformation as it slides. The plowing motion on the counterface produces a unique configuration. Plastic distortion is visible at the edge of the groove. An abrasive wear mechanism is indicated. The abrasive action of counterface asperities eliminates the matrix surrounding the particles. Upon sliding, particles are extracted and lodged among the specimens and the opposing surface. The aggregation of particles causes the two-body abrasion to transition into a three-body abrasion. Consequently, by emphasizing rolling friction rather than sliding friction, the wear rate of the on-site composites is decreased.

In contrast to the plate-like wear debris of the matrix alloy, the fine spherical particles generated by the three-body abrasion are smaller. The redistribution and morphological modification of Al_3Ni particles across the FSP raise rolling friction and the amount of worn debris. Materials deteriorate more slowly as a result, and the size of the particles produced by the degradation is decreased. These results are similar to those of Kishan et al., [35]. A tribomechanical mixed layer lowers the wear rate and shifts it from two-body to three-body wear by functioning as a solid lubricant. It was evident that the wear tracks in the base metal Al alloy were bigger than those in the Al-TiB_2 surface nanocomposites because of the hard TiB_2 particles present. However, the non-appearance of TiB_2 particles causes the surface that comes into contact with it to micro-plough up during wear, resulting in an uneven surface consistent with other researchers findings [36].

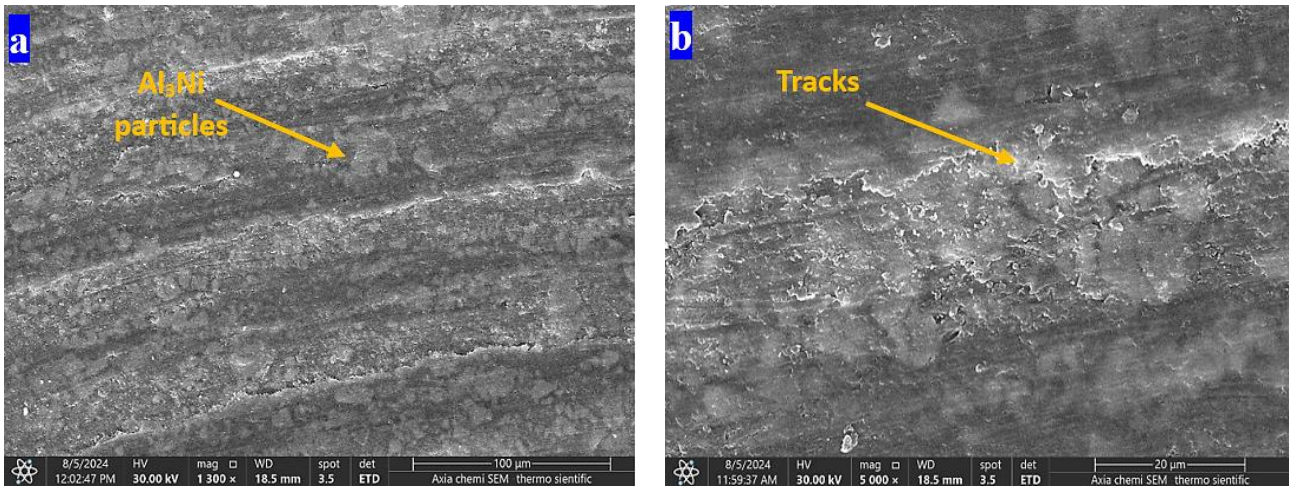

Figure 10: SEM micrographs for the worn surface of FSP A356/Al3Ni after the wear test at a load of 20N for 20 min;(a) 100 µm, (b) 20 µm

3.3.3 Friction coefficient

The ratio of the normal force resisting two surfaces together to the frictional force that prevents them from moving is called the friction coefficient (μ). The Equation 1 that represents this ratio is:

$$\mu = \frac{F}{N} \quad (1)$$

where μ:is friction coefficient, F: is the resistance force of friction (N), N: is normal force (N).

Table 2 summarizes the friction coefficient for the base A356 and the FSP in-situ composites A356. Figures 11(a-d), 12(a-d), 13(a-d), and 14(a-d) show the friction factor profiles for the A356 and A365 in-situ composites before and after FSP, respectively. The friction process parameters were 5, 10, 15, and 20 N load, the friction speed of 250 rpm, and the friction time of 20 minutes. Figure 11(a-d) shows that the substantial changes in the friction coefficient during the first few seconds of the friction test caused the coefficient curve to rise and fall noticeably. As the friction test progresses, the friction coefficient rapidly decreases until it achieves a steady state with a specific value of μ. During the first friction period, the in-situ composite carries a higher load the tiny contact area between the friction surface and the in-situ composite results in low frictional resistance. FSP samples reported a lower average friction coefficient than the base alloy for A356 and the in-situ composite before FSP. The friction coefficient is determined by an interplay of roughness features on the surfaces in contact, which fluctuates within a defined range throughout the entire testing duration; this possibly results in variations in the friction coefficient within a small range for every material as sliding distance increases. The friction coefficient decreases due to a smaller contact area, and the surface is protected from abrasions and scratches. This is probably one reason for the observed increase in the A356 in-situ composite's wear resistance after FSP. As seen in Table 2, the friction coefficient for all samples decreases as the load increases because of the increased work hardening of the worn surfaces at loads of 5-15 N. However, at a 20 N load, the base alloy friction coefficient and the in-situ composites with 15% nickel increase again after FSP. These results are similar to those of Srinivasu et al. [37], who found that a change in the wear process and lower friction coefficient values are associated with a higher resistance to wear of friction-stir-processed alloy and are consistent with the findings of previous researchers [38, 39]. There is very little frictional resistance in such cases.

Table 2: Friction coefficient of A356 and the FSP in-situ composites A356

Sample	5N	10N	15N	20N
A356 as cast	0.76	0.52	0.31	0.35
A356 after FSP	0.5	0.4	0.32	0.25
In-situ composite 15%Ni	0.55	0.45	0.28	0.20
In-situ composite 15% Ni after FSP	0.51	0.39	0.25	0.38

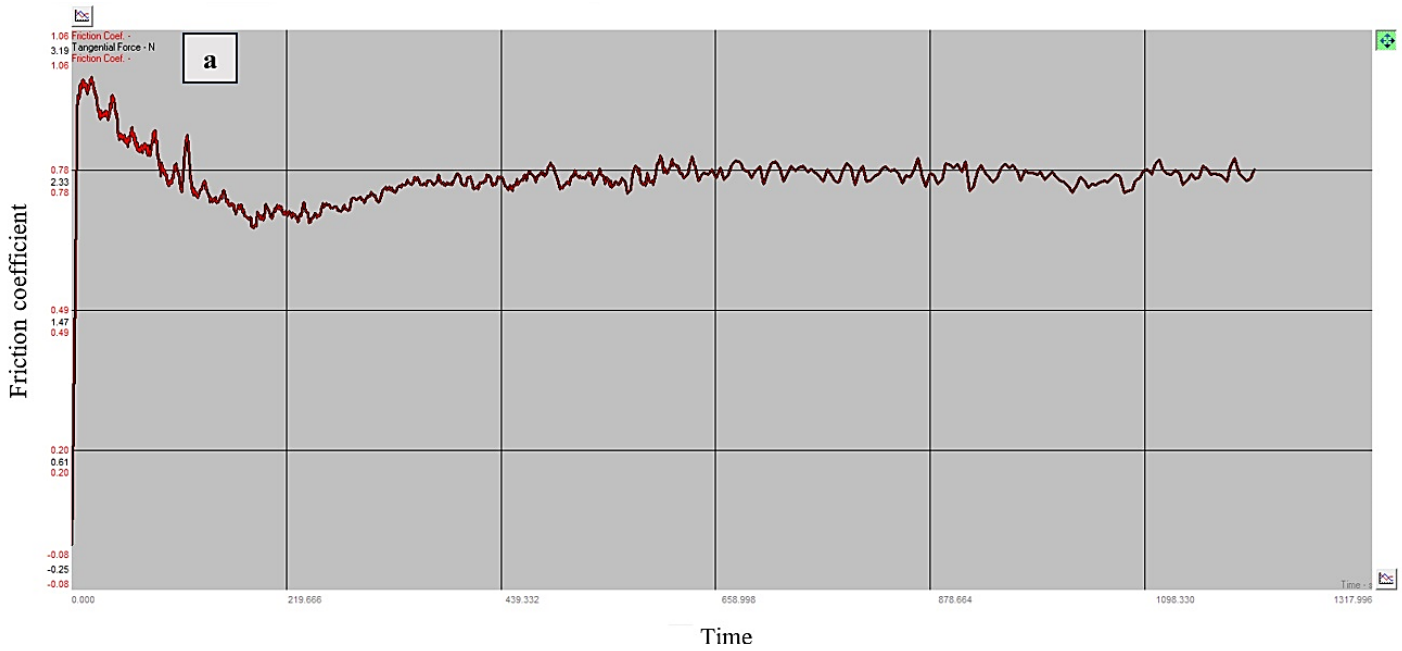

Figure 11: Coefficient of friction time function for as-cast A356 before FSP at different load (a) 5N (b) 10N (c)15N (d) 20N

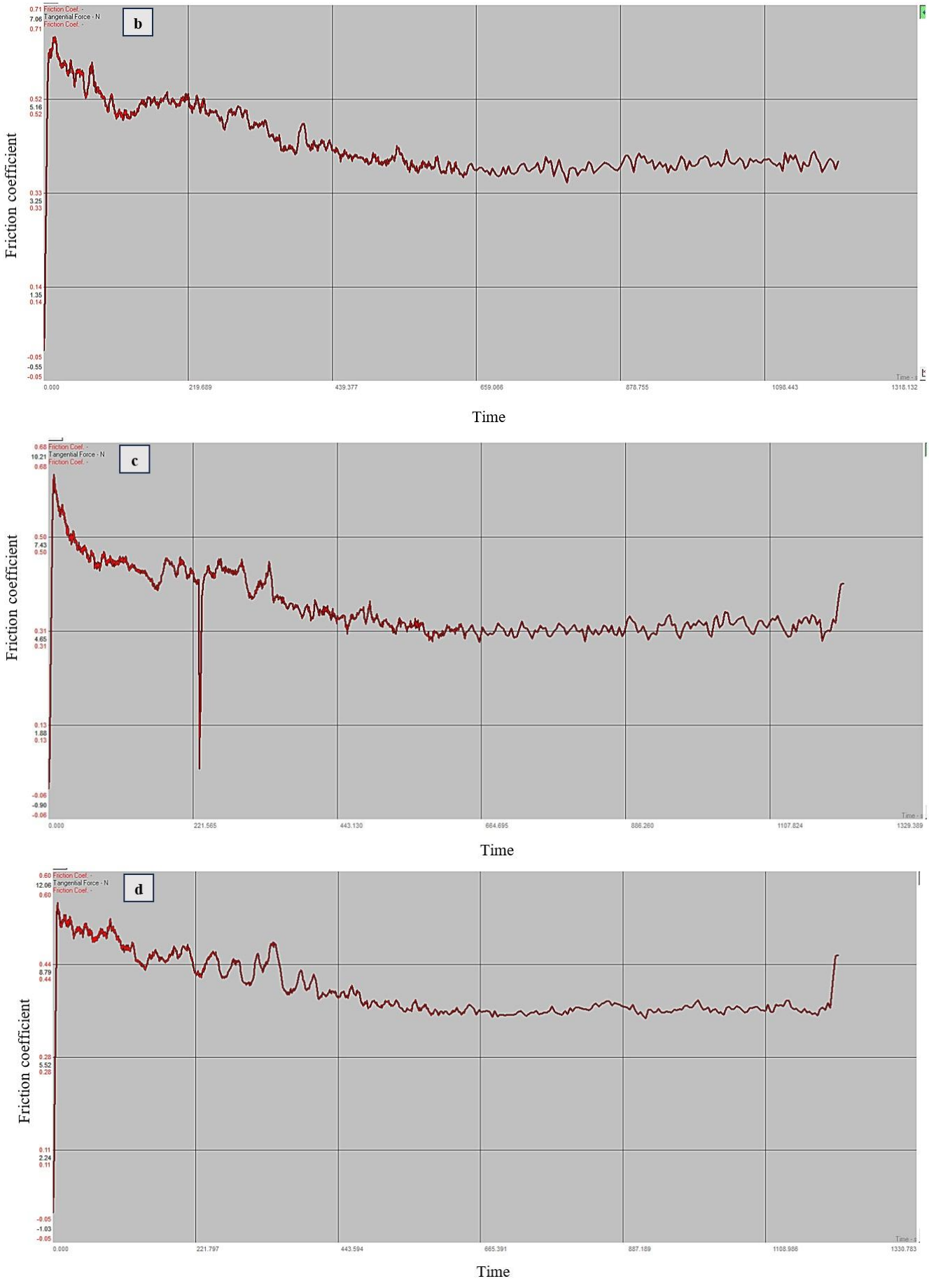

Figure 11: Continued

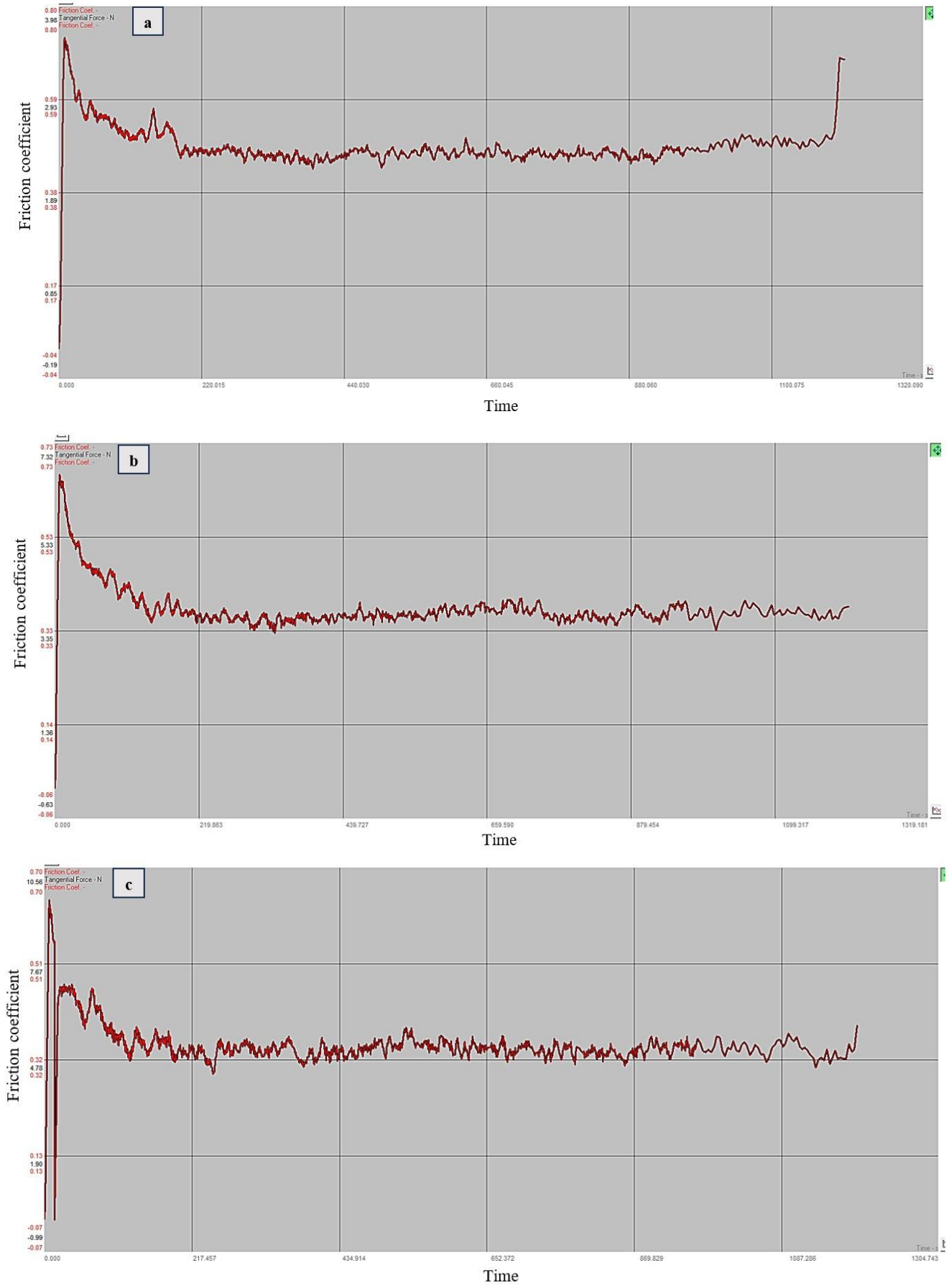

Figure 12: Coefficient of friction as time function for as cast A356 after FSP at different load (a)5N (b)10N (c)15 N (d)20 N

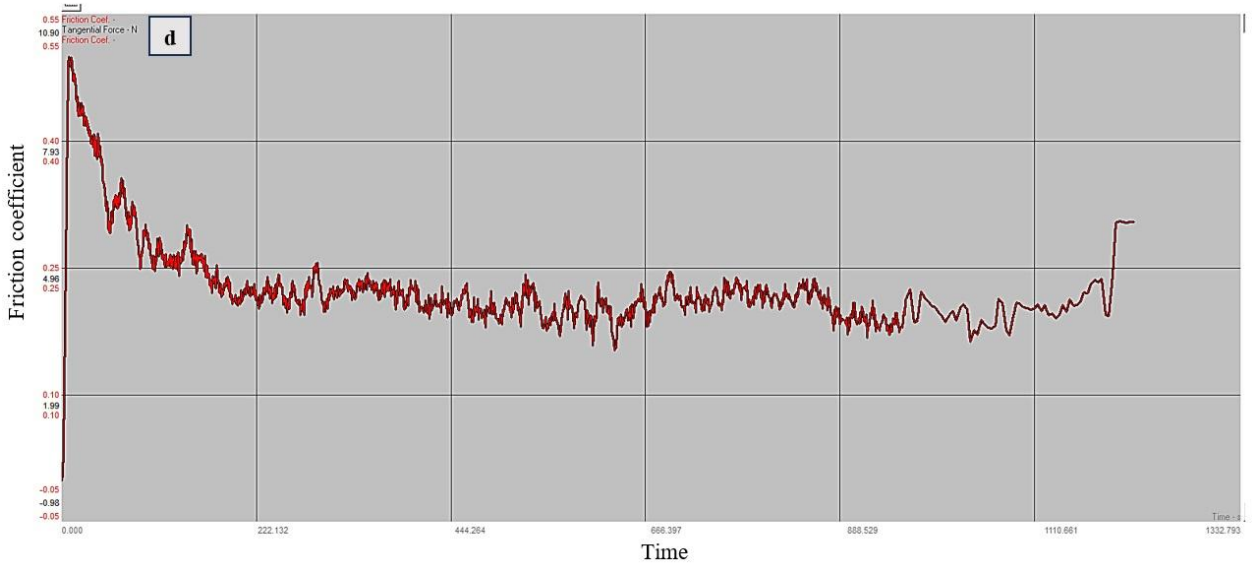

Figure 12: Continued

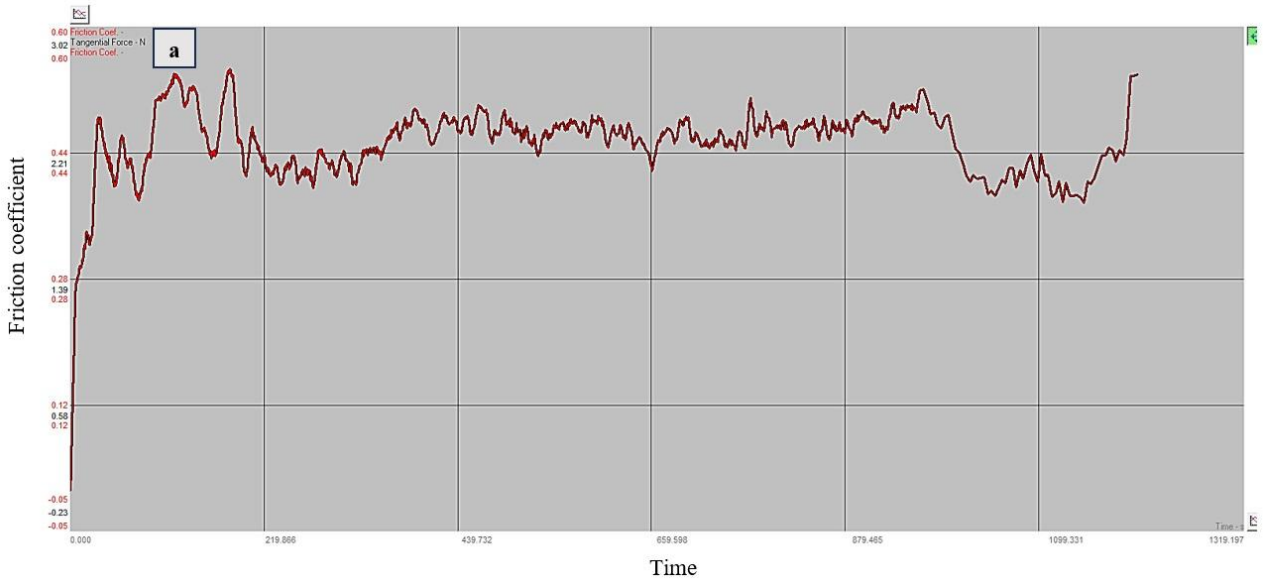

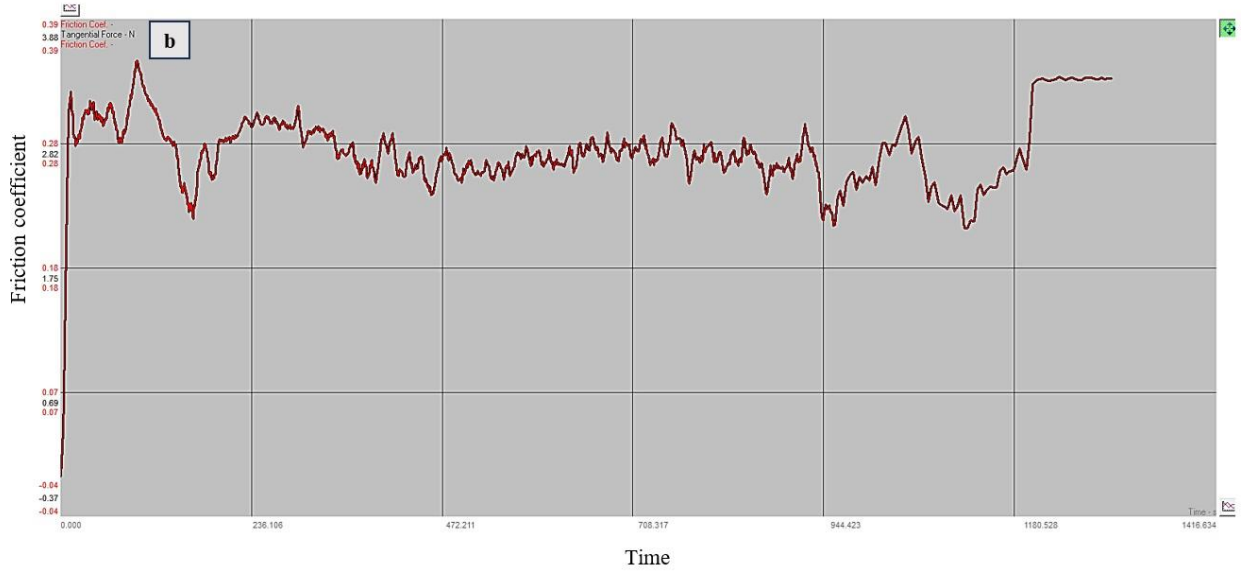

Figure 13: Coefficient of friction as a function of time for cast A356 in-situ composite before FSP at different load (a) 5N (b)10N (c) 15N (d) 20N

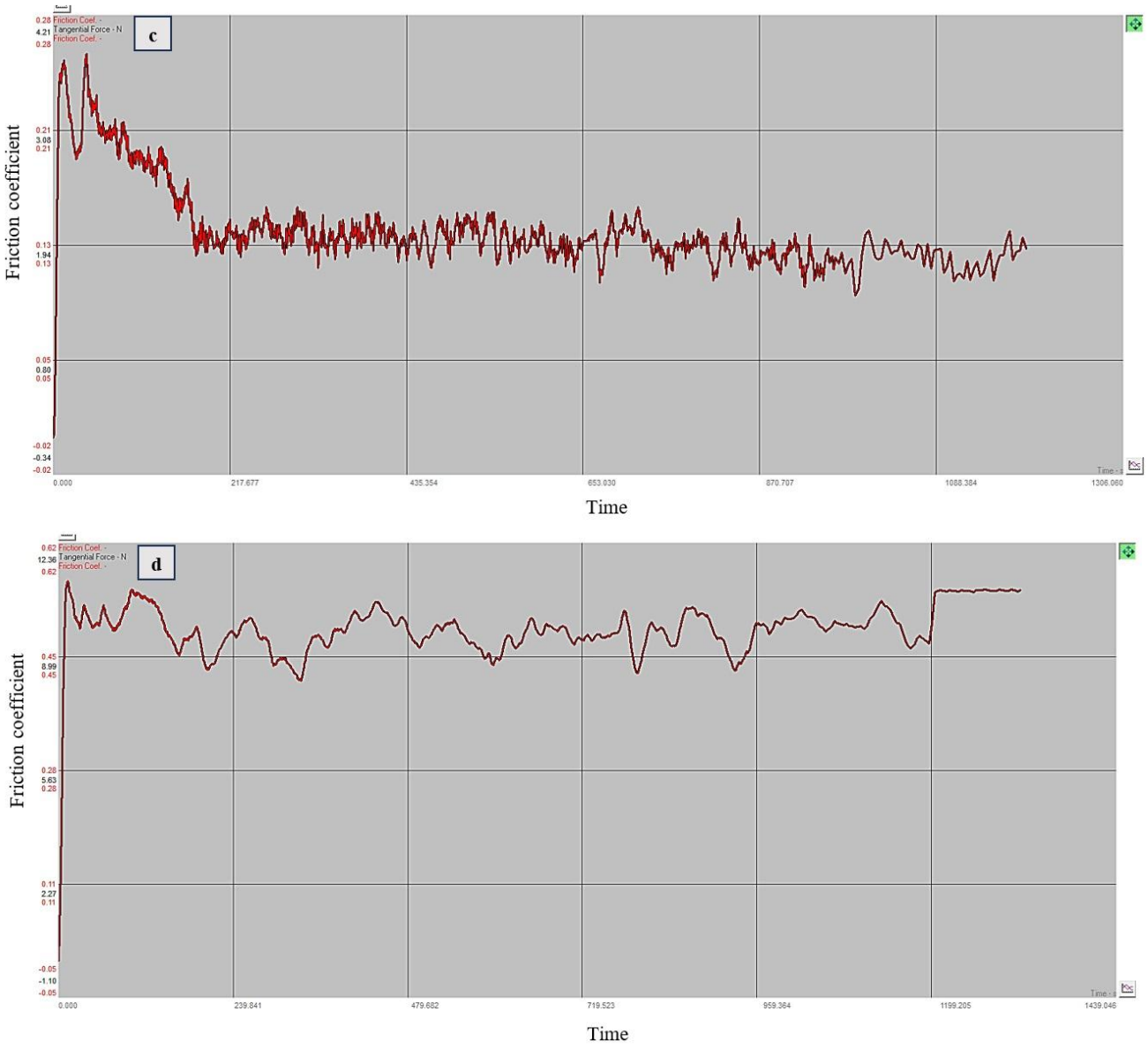

Figure 13: Continued

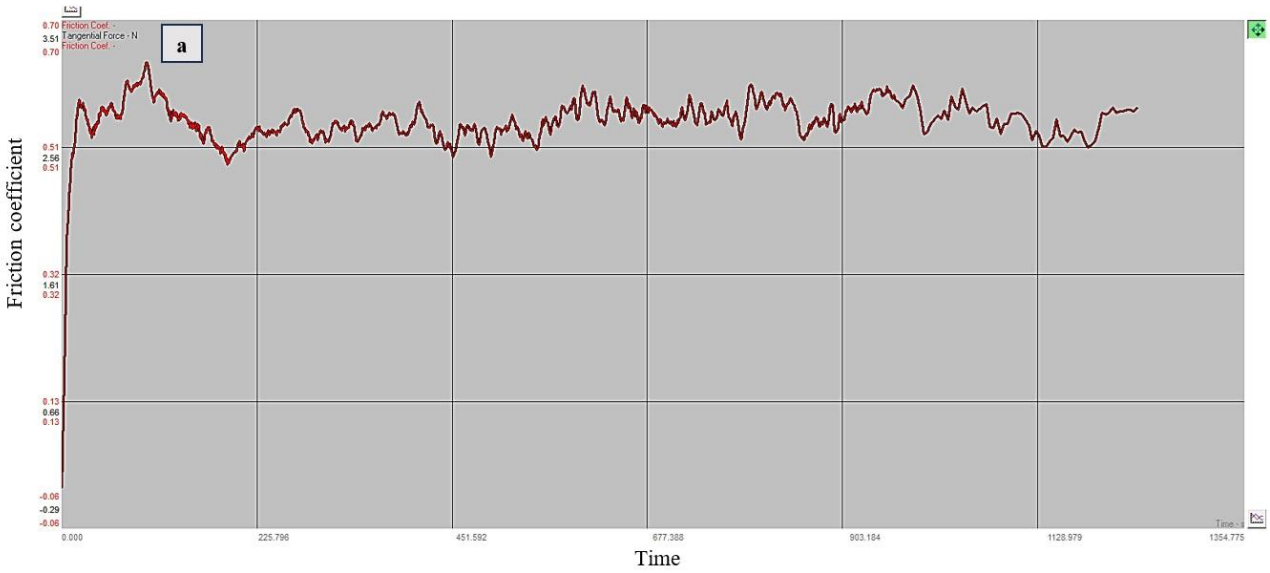

Figure 14: Coefficient of friction as a time function for cast A356 in-situ composite after FSP at different load (a) 5N (b) 10N (c)15N (d) 20N

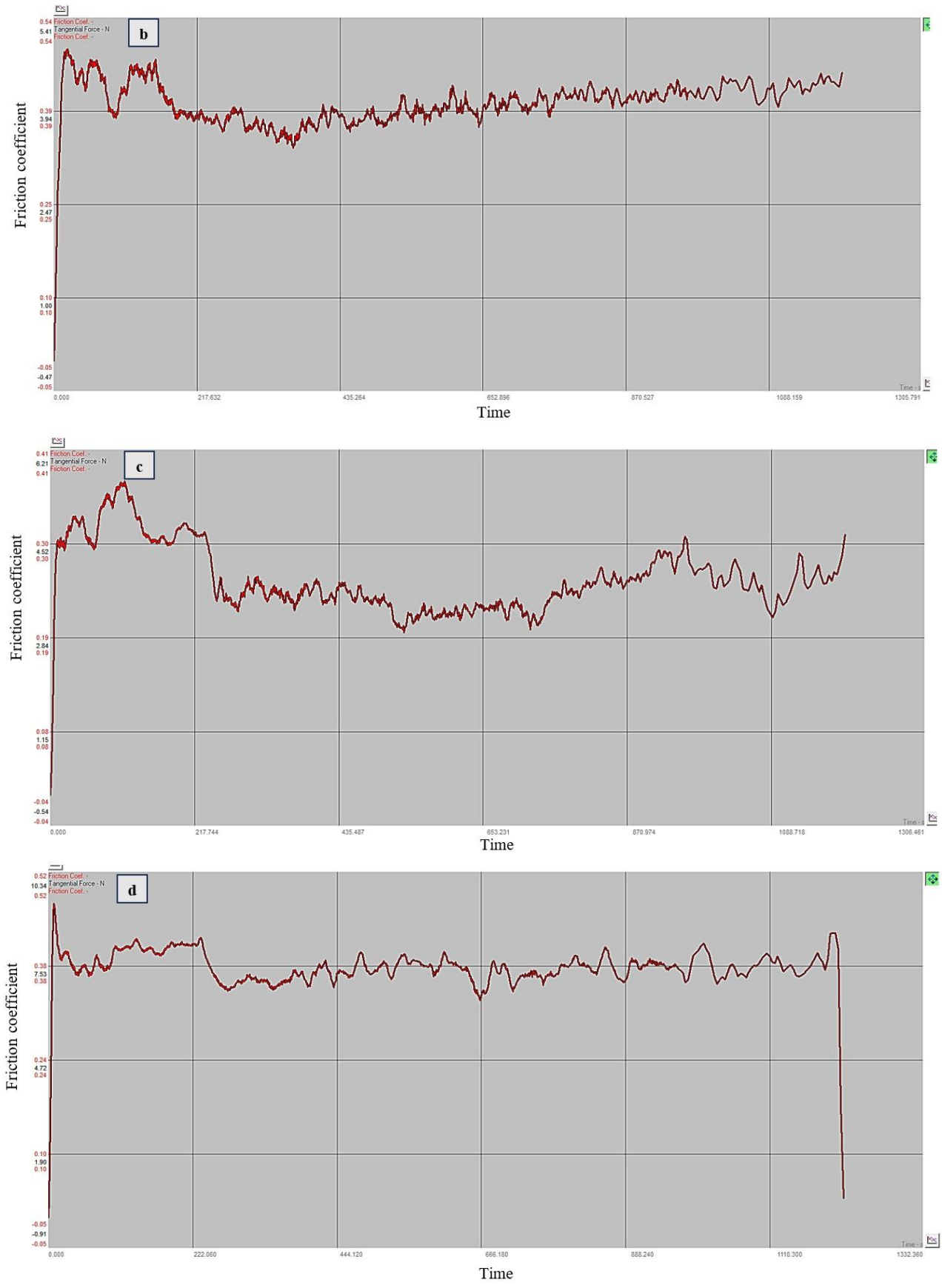

Figure 14: Continued

4. Conclusion

This work yields the following set of important conclusions:

1) Modification and microstructure refinement were observed in the in-situ composite and base alloy A356 after friction stir processing (FSP).
2) FSP enhanced the hardness of the basic alloy A356 and the in-place composite A356/Al_3Ni (87, 173 HV) due to frictional heating and plastic deformation in the FSP area.
3) FSP improved the distribution of intermetallic compound Al_3Ni particles in the Al-matrix and Si particles, resulting in a much smaller and homogeneous distribution in the A356 alloy matrix.
4) Numerous strengthening techniques transpired in the base alloy and on-site composites, including dispersion hardening through the formation of intermetallic phases of Al_3Ni particulates, grain boundary hardening via dynamic recovery and recrystallization in the SZ, and severe plastic deformation in both the SZ and the TMAZ, which significantly enhanced the mechanical characteristics.
5) It was found from the wear test that the wear behavior changes from mild wear at lower loads (5 N) to severe wear at higher loads (20 N).
6) During wear testing, the friction coefficient decreased as the applied load increased for the base A356 alloy and in-situ composite (A356/Al_3Ni).

Author contributions

Conceptualization, **N. Baheer , M. Abbass, I. Aziz** and **F. Khoshnaw**; data curation, **I. Aziz** ; formal analysis, **F. Khoshnaw** ; investigation, **N. Baheer** ; methodology, **N. Baheer** ; project administration, **N. Baheer**., resources, **M. Abbass** ; supervision, **M. Abbass** and **I. Aziz**; validation**, M. Abbass** and **I. Aziz**; visualization, **N. Baheer, M. Abbass** and **I. Aziz**; writing—original draft preparation, **N. Baheer**; writing—review and editing, **M. Abbass** and **I. Aziz**. All authors have read and agreed to the published version of the manuscript.

Funding

This research received no specific grant from any funding agency in the public, commercial, or not-for-profit sectors.

Data availability statement

The data that support the findings of this study are available on request from the corresponding author.

Conflicts of interest

The authors declare that there is no conflict of interest.

References

[1] R. Pratip, S. Singh, and K. Pal, Enhancement of mechanical and tribological properties of SiC and CB-reinforced aluminum 7075 hybrid composites through friction stir processing, Adv. Compos. Mater., 28 (2019) 1-18. https://doi.org/10.1080/09243046.2017.1405596

[2] E. Efzan, M. Noor, N. Siti Syazwani, and A Mustafa Al Bakri, Fabrication method of aluminum matrix composite (AMCs): a review, Key Eng. Mater., 700 (2016) 102-110. https://doi.org/10.4028/www.scientific.net/KEM.700.102

[3] A. Mussatto, I. U. Ahad, R. T. Mousavian, Y. Delaure, D. Brabazon, Advanced production routes for metal matrix composite, Eng. Rep., 3 (2021) e12330. https://doi.org/10.1002/eng2.12330

[4] V. S. Ayar and M. P. Sutaria, Comparative Evaluation of Ex Situ and In Situ Method of Fabricating Aluminum/Tib_2 Composites, Int. J. Met., 15 (2021) 1047-1056. https://doi.org/10.1007/s40962-020-00554-8

[5] N. Hoang Viet, N. Hoang Oanh, Microstructure and Electrical Property of Ex-Situ and In-Situ Copper Titanium Carbide Nanocomposites, Metals, 10 (2020) 1-10. https://doi.org/10.3390/met10060735

[6] M. Kumar Sahu, and R. Kumar Sahu, Fabrication of Aluminum Matrix Composites by Stir Casting Technique and Stirring Process Parameters Optimization, Advanced Casting Technologies, (2018) 111-122. https://doi.org/10.5772/intechopen.73485

[7] G. Atxaga, A. Pelayo, A. Irisarri, Effect of microstructure on fatigue behaviour of cast Al–7Si–Mg alloy, Mater. Sci. Technol., 17 (2001) 446-450. https://doi.org/10.1179/026708301101510023

[8] M. Santella, T. Engstrom, D. Storjohann, T.-Y. Pan, Effects of friction stir processing on mechanical properties of the cast aluminum alloys A319 and A356, Scr. Mater., 53 (2005) 201-206. https://doi.org/10.1016/j.scriptamat.2005.03.040

[9] Z. Ma, R.S. Mishra, M.W. Mahoney, Superplasticity in cast A356 induced via friction stir processing, Scr. Mater., 50 (2004) 931-935. https://doi.org/10.1016/j.scriptamat.2004.01.012

[10] S. Mohit Kumar, S. Raj Kumar, Fabrication of aluminum matrix composites by stir casting technique and stirring process parameters optimization, Adva. Cast. Technol., (2018) 111-122. https://doi.org/10.5772/intechopen.73485

[11] H. H. Zamel, S. Al-Ezzi, M. K Abbass, H. Soliman, Y. Zeng, Fabrication of AZ31/ZnO surface composite by friction stir processing: Evolution of microstructure, mechanical properties and corrosion behavior, Adv. Sci. Technol. Res. J., (5) (2025) 213-223. https://doi.org/10.12913/22998624/202274

[12] S. M. Aktarer, D. M Sekban, H. Yanar and G. Purçek, Effect of friction stir processing on tribological properties of Al-Si alloys, IOP Conference Series: Mater. Sci. Eng., IOP Publishing, 174 (2017) 1-8. https://doi.org/10.1088/1757-899X/174/1/012061

[13] H. Kumar, R. Prasad, P. Kumar, S. P. Tewari, J. K. Singh, Mechanical and tribological characterization of industrial wastes reinforced aluminum alloy composites fabricated via friction stir processing, J. Alloys Compd., 831 (2020) 154832. https://doi.org/10.1016/j.jallcom.2020.154832

[14] H. Daneshifar, A. Papi, M. Alishahi, Fabrication of Al-Si/Mg2Si in-situ composite by friction stir processing, Mater. Letter., 282 (2021) 128832. https://doi.org/10.1016/j.matlet.2020.128832

[15] P. Samal, B. Surekha, P. R. Vundavilli, Experimental Investigations on Microstructure, Mechanical Behavior and Tribological analysis of AA5154/SiC Composites by Stir Casting, Silicon, 14 (2022) 3317-3328. https://doi.org/10.1007/s12633-021-01115-2

[16] S. K. Gautam, S. K. Samanta, M. Mallik, H. Roy, A.K. Lohar, Wear and Mechanical Properties of In situ A356/5%Tib2 Composite Synthesis by Cooling Slope Technique, Int. J. Met., 17 (2022) 2239-2251. https://doi.org/10.1007/s40962-022-00931-5

[17] V. Singhal, VK Jain, RS Raman, D Patharia, V Mittal, S Mishra, H Kumar, Optimization of friction stir processing parameters for improving structural and mechanical properties in in-situ AA5083-H111/Al–Fe composites, Proceedings of the Institution of Mechanical Engineers, Part C: J. Mech. Eng. Sci., 238 (2023) 4477-4490. https://doi.org/10.1177/09544062231211672

[18] V. Rubtsov, A Chumaevskii, A Gusarova, E Knyazhev, D Gurianov, A Zykova, T Kalashnikova, Macro-and microstructure of in situ composites prepared by friction stir processing of AA5056 admixed with copper powders, Materials, 16 (2023) 1-21. https://doi.org/10.3390/ma16031070

[19] K. K. Jlood, M. K. Abbass, M. M. Hanoon, Effect of Friction Stir Processing Parameters on Microstructure and Mechanical Properties of Aluminum Alloy AA6061-T6: Experimental and Statistical Study , Salud Cienc. Tecnol. - Ser. Conf., 3 (2024) 862-862. https://doi.org/10.56294/sctconf2024862

[20] Z. Y. Ma, S. R. Sharma, R.S. Mishra, Effect of friction stir processing on the microstructure of cast A356 aluminum, Mater. Sci. Eng., A, 433 (2006) 269-278. https://doi.org/10.1016/j.msea.2006.06.099

[21] S. Senthil, M. Raguraman, D. T. Manalan, Manufacturing processes & recent applications of aluminum metal matrix composite materials: A review, Mater. Today Proc., 45 (2021) 5934-5938. https://doi.org/10.1016/j.matpr.2020.08.792

[22] N. A. Baheer, M. K. Abbass, I. A. Aziz, Effect of Friction Stir Processing on Microstructure and Mechanical Properties of In-Situ Composite A356/Al3Ni Fabricated by Stir Casting, Int. J. Comput. Methods Exp. Meas., 12 (2024) 453-461. https://doi.org/10.18280/ijcmem.120414

[23] Y. Zhao, X. Kai, G. Chen, W. Lin, C. Wang, Effects of friction stir processing on the microstructure and superplasticity of in situ nano-ZrB_2/2024Al composite, Prog. Nat. Sci. Mater. Int., 26 (2016) 69-77. https://doi.org/10.1016/j.pnsc.2016.01.009

[24] P. A. Kumar, H. C. Madhu, A. Pariyar, C. S. Perugu, S. V. Kailas, U. Garg, P. Rohatgi, Friction stir processing of squeeze cast A356 with surface compacted graphene nanoplatelets (GNPs) for the synthesis of metal matrix composites, Mater. Sci. Eng., 769 (2020) 1-23. https://doi.org/10.1016/j.msea.2019.138517

[25] I. Dinaharan, G. A. Kumar, S. J. Vijay, N. Murugan, Development of Al_3Ti and Al_3Zr intermetallic particulate reinforced aluminum alloy AA6061 in situ composites using friction stir processing, Mater. Design, 63 (2014) 213-222. https://doi.org/10.1016/j.matdes.2014.06.008

[26] M. H. Mohammed, A. D. Subhi, Exploring the influence of process parameters on the properties of SiC/A380 Al alloy surface composite fabricated by friction stir processing, Eng. Sci. Technol. Int. J., 24 (2021) 1272-1280. https://doi.org/10.1016/j.jestch.2021.02.013

[27] A. Kurt, I. Uygur, E. Cete, Surface modification of aluminium by friction stir processing, J. Mater. Process. Technol., 211 (2011) 313-317. https://doi.org/10.1016/j.jmatprotec.2010.09.020

[28] M. K. Abbass, Effect of Cd on microstructure and dry sliding wear behavior of (Al-12% Si) alloy, J. Eng. Res., 7 (2010) 1-10. https://doi.org/10.24200/tjer.vol7iss1pp1-10

[29] M. K. Abbass, N. A. Baheer, Effect of SiC Particles on microstructure and wear behavior of AA6061-T6 aluminum alloy surface composite fabricated by friction stir processing, In IOP Conf. Ser. Mater. Sci. Eng., 671(2020) 1720-1732. https://doi.org/0.1088/1757-899X/671/1/012159

[30] M. K. Abbass, M. J. Fouad, Study of Wear Behavior of Aluminum Alloy Matrix Nano Composites Fabricated by Powder Technology, Eng. Technol. J., 32 (2014) 1720-1732. https://doi.org/10.30684/etj.32.7A9

[31] M. J. Fouad, M. K. Abbass, I. Inanc, Manufacture of Self-Lubricating Mechanical Parts from Al-Si Alloy Matrix Hybrid Nanocomposites, Tribol. Ind., 47 (2025) 112-124. https://doi.org/10.24874/ti.1752.09.24.02

[32] A. O. Shiba, S. S. Mohamed, T. S. Mahmoud, Influence of Friction Stir Processing on the Microstructural, Hardness and Tribological Characteristics of A356 Cast Aluminum Alloy, Chars., (2018) 24-31.

[33] N. A. Baheer, M. K. Abbass, I. A. Aziz, Microstructure and Wear Behavior of In-situ Composite A356/Al3Ni Fabricated by Stir Casting, AIP Conference Proceedings, 3229, 2024, 070030. https://doi.org/10.1063/5.0236495

[34] M. K. Abbass, N. B. Sharhan, Characteristics of Al6061-SiC-Al_2O_3 surface hybrid composites fabricated by friction stir processing, J. Mater. Eng. Struct., 4 (2023) 147-158. https://doi.org/10.61552/JME.2023.04.002

[35] V. Kishan, A. Devaraju, K. P. Lakshmi, Influence of volume percentage of NanoTiB_2 particles on tribological & mechanical behaviour of 6061-T6 Al alloy nano-surface composite layer prepared via friction stir process, Def. Technol., 13 (2016) 1-6. https://doi.org/10.1016/j.dt.2016.11.002

[36] M. K. Abbass, Laser Surface Treatment and Modification of Aluminum Alloy Matrix Composites, Lasers Manuf. Mater. Process., 5 (2018) 81-94. https://doi.org/10.1007/s40516-018-0054-6.

[37] R. Srinivasu, A. S. Rao, G. M. Reddy, K. S. Rao, Friction stir surfacing of cast A356 Aluminum-silicon alloy with boron carbide and molybdenum disulphide powders, Def. Technol., 11 (2014) 1-18. https://doi.org/10.1016/j.dt.2014.09.004

[38] A. M. Al-Qutub, A. Khalil, N. Saheb, A. S. Hakeem, Wear and friction behavior of Al6061 alloy reinforced with carbon nanotubes, Wear, 297 (2013) 752-761. https://doi.org/10.1016/j.wear.2012.10.006

[39] M. K. Akbari, S. Rajabi, K. Shirvanimoghaddam, H. Baharvandi, Wear and friction behavior of nanosized TiB_2 and TiO_2 particle-reinforced casting A356 aluminum nanocomposites: A comparative study focusing on particle capture in matrix, J. Compos. Article Mater., 49 (2015)1-17. https://doi.org/10.1177/0021998314568327